

D. Harting, S. Wiesen, H. Frerichs, P. Boerner, D. Reiter, Y. Feng,
and JET-EFDA contributors

Application of the 3D Edge Code
EMC3-EIRENE to JET Single Null
Configurations by Validating Against
2D Simulations with
EDGE2D-EIRENE

“This document is intended for publication in the open literature. It is made available on the understanding that it may not be further circulated and extracts or references may not be published prior to publication of the original when applicable, or without the consent of the Publications Officer, EFDA, Culham Science Centre, Abingdon, Oxon, OX14 3DB, UK.”

“Enquiries about Copyright and reproduction should be addressed to the Publications Officer, EFDA, Culham Science Centre, Abingdon, Oxon, OX14 3DB, UK.”

The contents of this preprint and all other JET EFDA Preprints and Conference Papers are available to view online free at www.iop.org/Jet. This site has full search facilities and e-mail alert options. The diagrams contained within the PDFs on this site are hyperlinked from the year 1996 onwards.

Application of the 3D Edge Code EMC3-EIRENE to JET Single Null Configurations by Validating Against 2D Simulations with EDGE2D-EIRENE

D. Harting¹, S. Wiesen¹, H. Frerichs¹, P. Boerner¹, D. Reiter¹, Y. Feng²,
and JET-EFDA contributors*

JET-EFDA, Culham Science Centre, OX14 3DB, Abingdon, UK

Max-Planck Institut für Plasmaphysik, Association EURATOM, D-17491 Greifswald, Germany.

¹*Institut für Energieforschung – Plasmaphysik, Forschungszentrum Jülich, TEC, Association EUR-
ATOM -FZJ, D-52425 Jülich, Germany.*

²*Max-Planck Institut für Plasmaphysik, Association EURATOM, D-17491 Greifswald, Germany.*

** See annex of F. Romanelli et al, “Overview of JET Results”,
(Proc. 22 nd IAEA Fusion Energy Conference, Geneva, Switzerland (2008)).*

Preprint of Paper to be submitted for publication in Proceedings of the
19th International Conference on Plasma Surface Interactions, San Diego, California, USA.
(24th May 2010 - 28th May 2010)

ABSTRACT

The 3D Monte Carlo code EMC3-EIRENE[1] was successfully adapted to the single null configuration of JET. A test bed with the well established 2D edge plasma code EDGE2D-EIRENE [2, 5] was generated for this configuration to check the adaptation of the EMC3-EIRENE code and isolate possible candidates for further improvement. As both codes solve the same set of fluid equations, even though using different solving techniques (respectively a Monte Carlo method in the EMC3 and a finite differences scheme in the EDGE2D code), the results should be very similar as both codes are coupled to the same kinetic neutral particle Monte Carlo code EIRENE[3] to simulate the plasma-neutral interaction. This paper will show that both codes are in a fairly good agreement regarding plasma profiles and even recycling regime.

1. INTRODUCTION

The EMC3-EIRENE code, which was originally developed for stellarator geometries of W7-AS and W7-X[7], is a Monte Carlo code which solves a set of time independent Braginskii fluid equations for the plasma edge. It has already successfully been used at TEXTOR-DED [8, 9], and was recently extended to deal with divertor geometries including X-point configurations[4]. This new development has already been applied and tested for the DIII-D tokamak. As a next step, the EMC3-EIRENE code was now also adapted to the JET environment to benchmark it against the at JET well established EDGE2D-EIRENE code, which is a 2D time dependent plasma edge fluid code using a finite difference scheme.

2. SIMULATION PARAMETERS

Even though the EMC3 code is a full 3D code which can also cope with ergodic magnetic field configuration, this comparison was done in a toroidal symmetric configuration to apply to the natural capabilities of the 2D code EDGE2D. The simulation domain of the EMC3-EIRENE code covers a toroidal segment of $\varphi = 22.5^\circ$ with a toroidal grid resolution of $n_{\text{tor}}=16$ and periodic boundary conditions. Although the EMC3 code [5], as well as the EDGE2D code, have parallel heat flux and viscosity limiters implemented, we used for simplicity reasons only the standard classical parallel heat conductivity and have switched off the parallel viscosity for the main comparison between the two codes. Only at the end, when we investigate the recycling regimes obtained by the two codes, we compared also the results with classical parallel viscosity and with no parallel viscosity.

Although we have tried to keep all settings the same in the two codes, the main physical differences between the EMC3-EIRENE and the EDGE2D-EIRENE model, which could not be brought in line, are the following:

- The EMC3-EIRENE code uses decay lengths λ_{Te} , λ_{Ti} as boundary conditions for electron and ion temperatures respectively. EDGE2D-EIRENE, however, uses the fractional change in temperature over the outermost two grid rings in the SOL as a boundary condition for the temperatures.
- The EDGE2D-EIRENE code uses the recombination of plasma ions calculated by EIRENE

as a particle sink. In the EMC3 code, this option is not yet implemented, but it should only be significant in very cold ($T_e < 5\text{eV}$) plasma regions like the private flux region of the divertor or in detached plasmas.

- The EDGE2D-EIRENE code uses also more molecular processes from EIRENE. These additional molecular processes will also be used in the future by the EMC3-EIRENE code, but at the moment, the focus is to detect the key processes and parameters and thus the input file for EIRENE was kept simple.

For the test bed, the Pulse No: 50401 with the magnetic equilibrium at 18.0s was chosen which had the strike points on the vertical targets being docile from the modelling point of view. The boundary conditions were set to typical JET L-mode parameters with the input power entering the simulation domain from the core set to $P_{\text{in}} = 3.5\text{MW}$. The particle decay length at the outer SOL boundary was set to $\lambda_n = 2.5\text{cm}$, the anomalous perpendicular transport coefficients for particles to $D = 0.3\text{m}^2\text{s}^{-1}$ and for the energy of electrons and ions to $\chi_e = \chi_i = 1\text{m}^2\text{s}^{-1}$ respectively. For the EMC3 code, the decay lengths for the temperature at the outer SOL boundary were also set to $\lambda_{T_e} = \lambda_{T_i} = 2.5\text{cm}$, however, the temperature drop parameters of the EDGE2D code were set to typical values of 2% for ions and 4.6% for electrons respectively.

In the next section, the modelling results of the two codes for a low and a high density case are shown. For the low density case (shown in red), the upstream density at the separatrix on the outer midplane was set to $0.49 \times 10^{19}\text{m}^{-3}$ and for the high density case (shown in blue) to $1.1 \times 10^{19}\text{m}^{-3}$.

3. SIMULATION RESULTS

In figure 1, the radial density profiles obtained by the EMC3-EIRENE and EDGE2D-EIRENE code at the Outer (OMP) and Inner (IMP) Midplane are shown. Outside of the separatrix, the profiles are in good agreement. At the inner core boundary, of the inner and outer midplane profiles, the density obtained by the EDGE2D code is nearly the same. However the density obtained by the EMC3 code drops about 3.4% (low density case) and 7.3% (high density case) from the outer midplane to the inner midplane. This arises from the fact that in the present simulations the EMC3 code weighted the influx through the core boundary into the simulation domain by the inverse distance of the flux surfaces, leading to a higher influx at the OMP compared to the IMP. The wiggle in the EMC3 density profile around $r = 0.08\text{m}$ for the high density case is due to statistical noise near the outer boundary. The Monte Carlo particles in the EMC3 code are generated at the core boundary and at volume sources and get constantly lost towards the target plates while they travel outwards. This means that the statistical noise gets worse moving radially outwards from the separatrix towards the outer boundary. This effect can also be seen in the radial ion temperature profile (fig.2) and the temperature profiles along the target plates (fig.5).

The simulation results of the radial electron and ion temperature profiles at the OMP are shown in figure 2. It is obvious that the results for the ion temperature of the two codes are in a good agreement. The stronger drop of the EMC3 ion temperature near the outer boundary ($r > 0.03\text{cm}$) is a result of

the different boundary conditions at the outer boundary of the two codes. The temperature drop parameter of the EDGE2D code for the ion temperature (2%) results in an effective decay length on the simulation boundary of $\lambda_{Ti,OMP} \approx 11\text{cm}$ at the OMP and of $\lambda_{Ti,IMP} \approx 19\text{cm}$ at the IMP, which is much higher than the decay length $\lambda_{Ti} = 2.5\text{cm}$ used by the EMC3 code. Regarding the electron temperature, the EMC3 code tends to give slightly lower temperatures than the EDGE2D code, especially inside of the separatrix. This behavior is confirmed in the electron and ion temperature profiles along the separatrix, which are shown in figure 3. Here the EMC3 code produces an electron temperature on the separatrix of approximately 20eV lower than the EDGE2D code for the low density case. This is an indication that the particle content is slightly higher in the EMC3 simulation. Nevertheless the electron temperature along the separatrix for the high density case and the ion temperatures along the separatrix for both density cases are in a very good agreement. The radial temperature profiles at the IMP show similar results as on the OMP wherefore we forgo to show these results here.

Regarding now the energy flux on the outer and inner targets in figure 4, the agreement between the EDGE2D and the EMC3 code, beside some slightly stronger peaked heat fluxes in the EDGE2D results is very good at the Outer Target (OT) for both density cases. Nevertheless, the Inner Target (IT) shows some significant differences. For the low density case, the EDGE2D code gives at the inner target a stronger peaked and by 50% higher heat flux than the EMC3 code, where in contrast for the high density case the EDGE2D heat flux on the IT is reduced by 50% compared to the results obtained by the EMC3 code. The reason for this asymmetry between the inner and outer target is not yet clear. Anyhow the electron and ion temperatures are still in a good accordance at the outer and inner target (see figure 5, inner target similar). Neglecting the statistical noise for distances larger than 17cm in the EMC3 results of figure 5, the biggest difference can be found for the electron temperature in the low density case. Here the EDGE2D code delivers a stronger peaked and by 30eV larger peak electron temperature.

The particle fluxes obtained by the EMC3 and the EDGE2D code for the low density cases at the inner and outer target (figure 6) are in a good conformance. However for the high density case, the particle flux from the EDGE2D code is stronger peaked and about 25% larger at the inner target and even 70% larger at the outer target. This is also reflected in a higher density along the inner and outer target which the EDGE2D code results for the high density case compared to the EMC3 code (figure 7). Regarding the density along the separatrix (figure 8), it points out that for the high density case, the plasma density directly in front of the target is in the EDGE2D results stronger peaked and nearly twice as high as the results obtained by the EMC3 code. This goes in line with the ionization profiles along the separatrix shown in figure 9. The ionization for the high density case of the EDGE2D-EIRENE result is 6 times larger at the inner target and even 30 times larger at the outer target compared to the EMC3-EIRENE results. The reason for this highly peaked ionization profiles at the targets compared to the EMC3_EIRENE ionization profiles is not completely clear. It could arise from the fact that the EDGE2D grid has a very high localized grid resolution near the divertor targets compared to the presently used EMC3 grid. The EDGE2D grid is locally near

the divertor target up to 4-5 times finer in perpendicular direction to the target and approximately two times finer parallel to the field line. Summing up the Monte Carlo particles in EIRENE on this coarser EMC3 grid, leads to a smoothening of the ionization profiles and therefore could be responsible for the less peaked ionization and density profiles.

Finally, the recycling regime for the low and high density case is analyzed. In this context a density scan has been performed with the EDGE2D-EIRENE code, and result is shown in figure 10. The density scan has been carried out for a case without parallel viscosity (red curve) and with classical parallel viscosity (green curve). For the case without parallel viscosity, it points out that up to an outer midplane separatrix density of about $6 \times 10^{18} \text{ m}^{-3}$ the EDGE2D-EIRENE code is operating in the linear sheath limited regime and for higher densities fades to the conduction limited high recycling regime. By adding the classical parallel viscosity to the simulation, the transition between the two regimes can be moved towards lower separatrix densities. The blue stars in figure 10 denote the above discussed high and low density case of the EMC3-EIRENE code. It is obvious that in the case without parallel viscosity the recycling regime of the EDGE2D-EIRENE code could be well reproduced with the EMC3-EIRENE code. The slightly higher recycling flux of the EMC3-EIRENE simulation for the low density case indicates a higher particle content compared to EDGE2-EIRENE simulation. This can also explain the lower electron temperature along and radially inside of the separatrix which were observed for the EMC3-EIRENE simulation compared to the EDGE2D-EIRENE results (figure 2 and 3).

CONCLUSIONS

The presented benchmark between the EDGE2D-EIRENE and the EMC3-EIRENE code for a single null divertor configuration proved that both codes are in a reasonably good agreement. The radial and parallel profiles of the plasma parameters match very well in line with the applied model parameters. Even the observed transition of the EDGE2D-EIRENE code into the high recycling regime could be well established also with the EMC3-EIRENE code. Only the strong decrease of the heat flux observed by the EDGE2D-EIRENE code for the high density case at the inner target could not be reproduced by the EMC3-EIRENE code. Nevertheless, this positive code comparison lays the foundation for further direct simulations of experimental related 3D dimensional effects in the SOL at JET, like for instance the recently observed strike point splitting obtained by resonant magnetic perturbation with the error field correction coils at JET [10].

ACKNOWLEDGEMENT

The views and opinions expressed herein do not necessarily reflect those of the European Commission. This work was supported by EURATOM and carried out within the framework of the European Fusion Development Agreement. The views and opinions expressed herein do not necessarily reflect those of the European Commission.

REFERENCES:

- [1]. Y. Feng, F. Sardei, J. Kisslinger, P. Grigull, K. McCormick and D. Reiter, Contribution Plasma Physics, **44** 1-3 (2004) 57-69.
- [2]. R. Simonini, G. Corrigan et al., Contribution Plasma Physics, **34** 2/3 (1994) 368-373.
- [3]. www.eirene.de
- [4]. H. Frerichs, D. Reiter, Y. Feng and D. Harting, Computer Physics Communications, **181** 1 (2010) 61-70.
- [5]. D. Harting, D. Reiter, Y. Feng, O. Schmitz, D. Reiser and H. Frerichs, Contribution Plasma Physics, **48** 1-3 (2008) 99-105.
- [6]. EDGE2D-EIRENE report
- [7]. Y. Feng W7-AS W7-X EMC3
- [8]. M. Kobayashi Textor-DED EMC3
- [9]. D.Harting Juel Report
- [10]. E. Nardon, Poster P1-43, this conference.

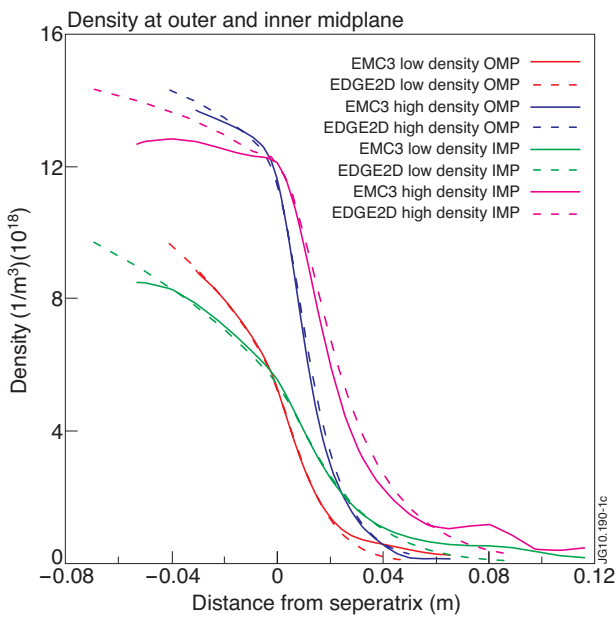


Figure 1: Radial density profiles at outer and inner midplane.

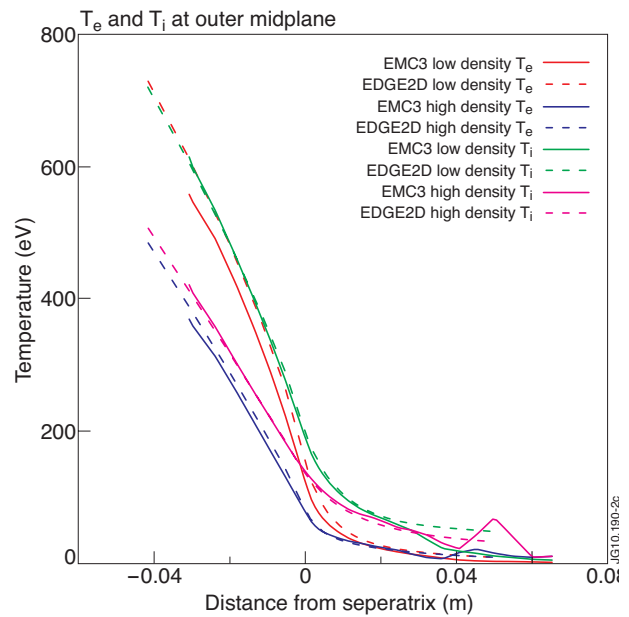


Figure 2: Radial electron and ion temperature profiles at outer midplane.

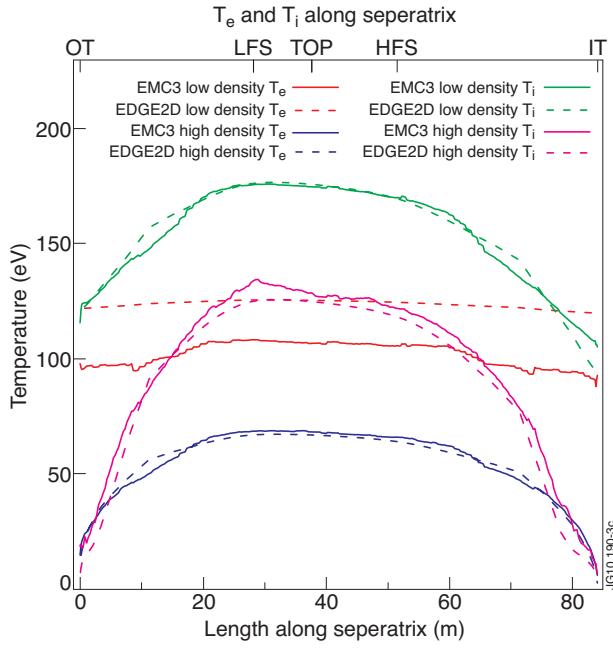


Figure 3: Parallel electron and ion temperature profiles along separatrix.

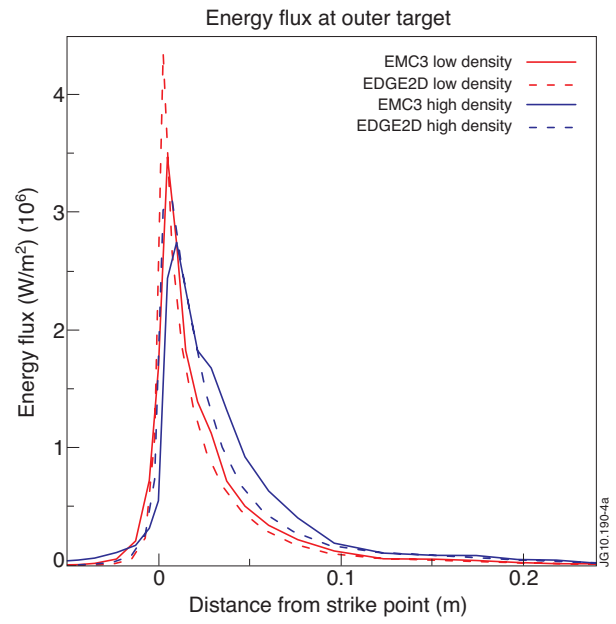


Figure 4: Energy flux on the inner (top) and outer (bottom) target.

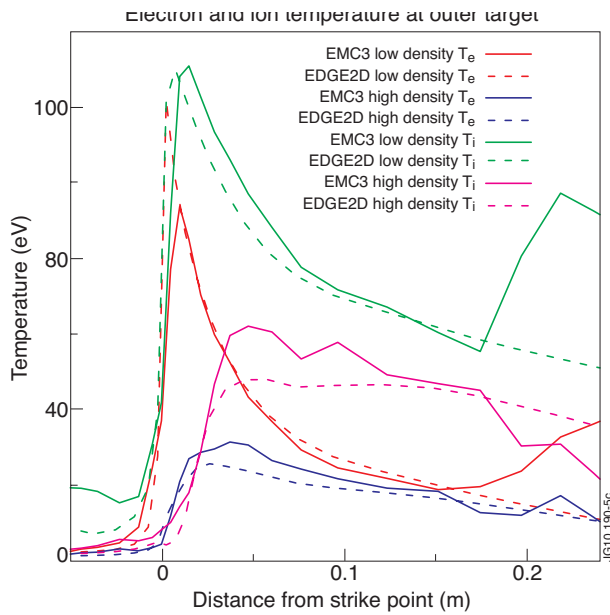


Figure 5: Electron and ion temperature profiles along the outer target.

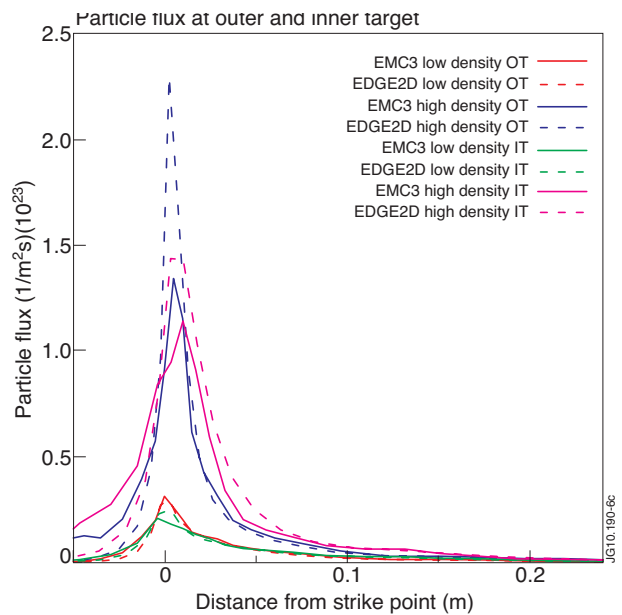


Figure 6: Particle flux on the inner and outer target.

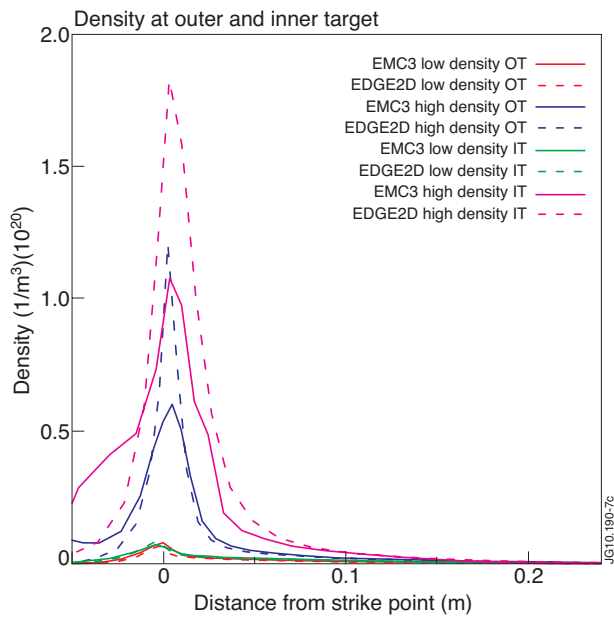


Figure 7: Density profiles along the inner and outer target.

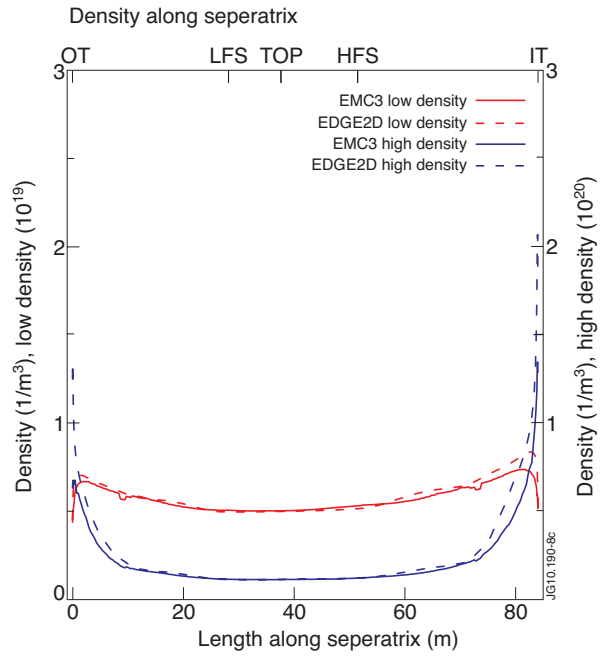


Figure 8: Parallel density profiles along the separatrix (the y-axis for the low density case is on the left and for the high density case on the right side).

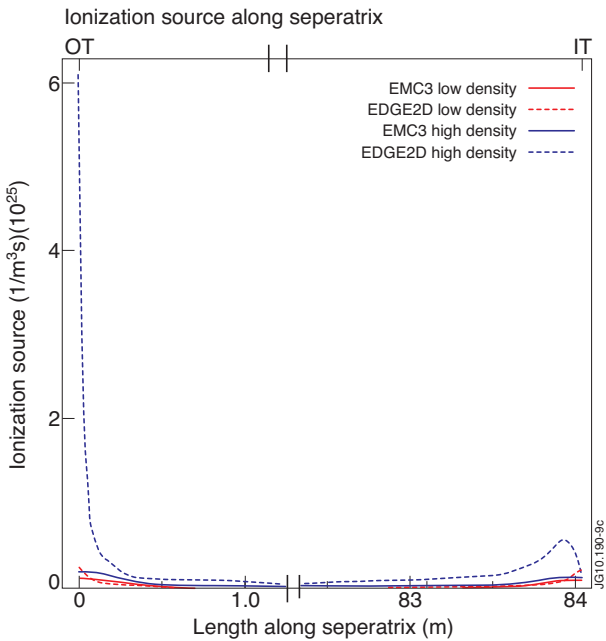


Figure 9: Ionization source along the separatrix (the y-axis for the low density case is on the left and for the high density case on the right side).

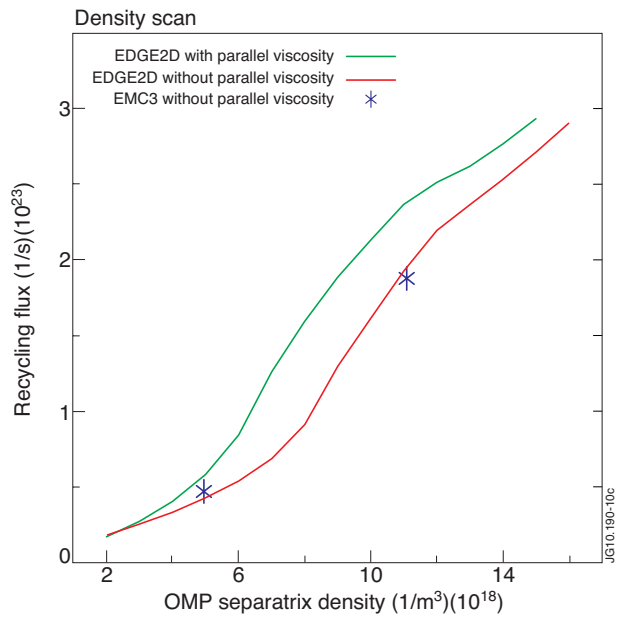


Figure 10: Density scans showing the recycling regime.